Maximizing GW-Detector Sensitivity through Brute Force Differential Evolution Optimization

Derek Hammar

31/07/2018

Preface

Contents

List of Figures

0 Introduction

Gravitational waves are a concept that has existed since 1893, and was shown to be theoretically possible in 1915 with the publication of Einstein's theory of general relativity. [1][2] Einstein doubted his own calculations, and tried to publish a paper discussing the incompatibility of gravitational waves with general relativity; however was convinced otherwise during the peer-review process.[2][3] Despite these predictions nobody was able to directly measure the effects of gravitational waves, and nobody would be able to for quite some time.

In order to measure the displacement of space, start with a Michelson Interferometer (Figure 1), originally used in the Michelson-Morley experiment disproving the existence of an ether wind. [4] The setup is relatively simple, the laser is sent to two mirrors via the beam splitter which then recombines the beams before sending them to the screen. When a gravitational wave is passing through, Mirror 1 (M1) will move either farther or closer to the Beam Splitter (BS) while Mirror 2 (M2) will do the opposite. [5] This means that the optical path length (OPL) of each beam will be different scaled by the amount that each mass moves. Since the OPL's are different the recombinant beam will produce some interference pattern on the screen. This interference pattern is the detection of a gravitational wave.[5]

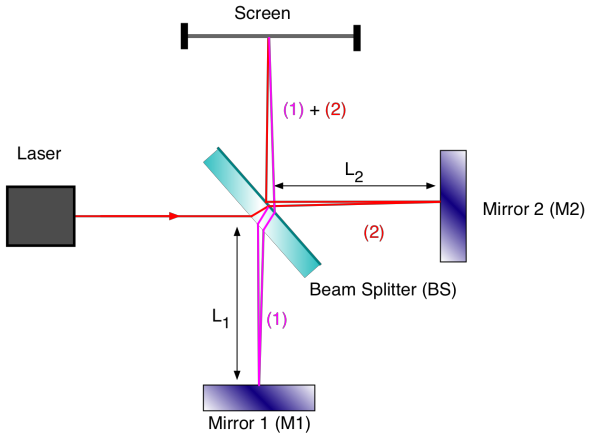

Figure 1: Simple Michelson Interferometer.

In order to grasp the magnitude of such a feat, its important to note that the sensitivity of this detector must be greater than 10^{-18} meters in order to detect anything at all. [5] Measuring such a infinitesimally small distance requires a good understanding of the noise involved since any change in distance resulting from thermal fluctuations, seismic vibrations, quantum noise and others can dramatically affect the sensitivity of the detector.

The aim of this project is to optimize the sensitivity of these detectors in the 1-3 kHz range, where the limiting factor is quantum noise (Figure 2), using a Modular and Adaptable Gravitational-wave Interferometer noise Calculator (MAGIC). This exercise will serve not only to validate MAGIC as a tool for analyzing GW-detector noise, but also to verify previous results found using the accepted Gravitational Wave Interferometer Noise Calculator (GWINC). Quantum noise will be discussed further in Section 2, and MAGIC will be discussed in Section 3.

1 Noise in Gravitation-Wave Detecting Interferometers

1.1 Introduction to Noise

There are many sources of noise that must be taken into account in GW-detectors only some will be discussed in depth here. Below is a brief description of the various sources of noise.

Seismic Noise Beginning with the low frequencies, one of the limiting factors is seismic noise. Seismic noise is the sum vibrations due to everything from human activities to earthquakes. [8] This noise is estimated by accelerators held in isolation with the masses. [8] Seismic noise is devastating at low frequencies, and is the reason that future detectors such as the Einstein telescope are planned to be underground. The ideal location would be in the isolation of space. [7]

Coating Thermo-optical Noise All test mass substrates are covered with an optical coating micrometers thick to optimize their reflectivity. This requirement introduces thermal noise from the mechanical losses of the coating and is far more limiting than substrate thermo-elastic noise. [8]

Coating Brownian The coating Brownian noise is the noise resulting from the statistical fluctuations in the coating due to its non-zero temperature. This noise can be reduced by reducing the temperature, and by looking into new materials. [9]

Substrate Thermo-elastic Noise is caused by the expansions and contractions within the masses due to temperature fluctuations. [8] Once again, a reduced temperature should reduce this noise, as well as implementation of new materials. For this reason ET-LF is planned to operate at 123 K since the thermal expansion passes through zero for silicon, one of the possible materials for the mass. The other possibilities are sapphire and fused silica. [11, 7]

Newtonian This noise is caused by the variations in the density of the surrounding earth. These variations lead to a fluctuating local gravitational field, affecting the movement of the masses. There are plans to combat this noise through a cancellation that measures real-time density fluctuations. [10]

Residual Gas Noise Residual gas noise is the least pressing noise source discussed. It results from the interactions of the beam with the small amounts of gas left in the vacuum chamber. This noise is not a limiting factor in any frequency bandwidth at this point in time. [8]

Quantum Noise Quantum noise will be the subject of section 1.2. In short, quantum noise is composed of two parts: Shot noise and radiation pressure. Shot noise generated from the fluctuations in photons striking the photo-diode due to the distribution of phases. [6] Radiation pressure is the noise generated by the momentum of the photons pushing on the mass.[6]

Substrate Brownian Noise Substrate Brownian noise will be the subject of Section 1.3. This noise is generated by the statistical fluctuations in the mass. While it is not a limiting factor, it is more prevalent in the low frequency range and will be greatly reduced in ET-LF through cryogenics and a change of substrate material. [7, 11]

A more in-depth description of both the quantum noise and substrate thermal noise is given in the following sections. Figure 2 shows the noise curve for aLIGO. The x-axis shows the frequency of the incoming gravitational wave as compared with the noise. The y-axis is more interesting because it seems odd to measure noise in such units. These units show how strong the noise is in terms of a gravitational wave signal. In other words it shows the strain of the gravitational wave required to produce a signal the same strength as the noise.

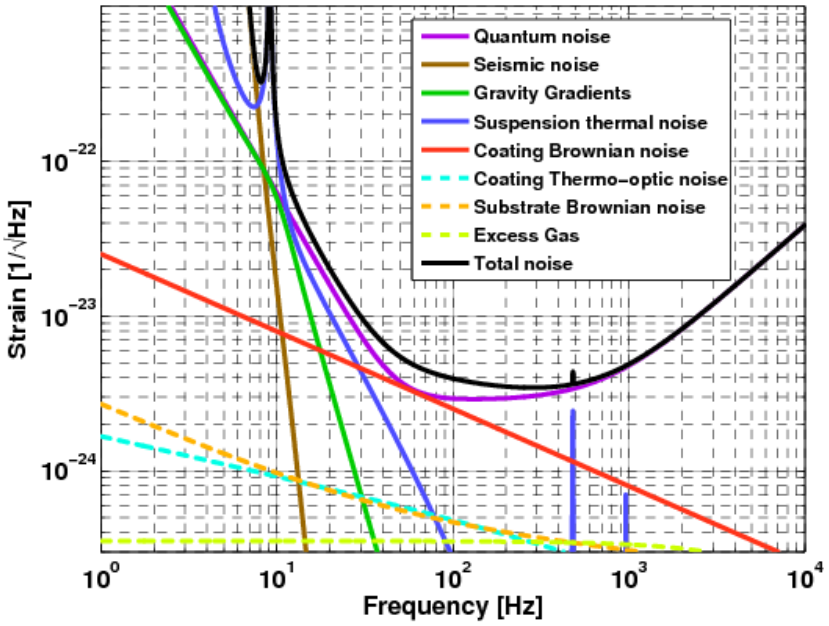

Figure 2: ALIGO Noise Curve.

.

1.2 Quantum Noise for a Simple Michelson Interferometer

The following will derive the quantum noise for a simple Michelson interferometer. Keep in mind that since the model does not include recycling cavities, there will be discrepancies with advanced interferometers. The most important ideas in the derivation are found in equation 6, showing the dual-component noise.

1.2.1 Derivation

The following derivation of Quantum noise will be following the procedure found in "Exploring Macroscopic Quantum Mechanics in Optomechanical Devices" (2010) Example 2.5.1 [6]. This will show the quantum noise for a simple Michelson interferometer (1), meaning there will be no signal or power recycling. The quantum mechanical formula for the electric field is given by:

$$\hat{E} = U(x,y,z)\int_0^\infty \frac{d\omega}{2\pi}\sqrt{\frac{2\pi\hbar\omega}{\mathcal{A}c}}[\hat{a}_\omega e^{ikz-i\omega t} + \hat{a}_\omega^\dagger e^{-ikz+i\omega t}] \tag{1}$$

As explained by Haixing Mao, "Here $\hat{a}_\omega$ and $\hat{a}_\omega^\dagger$ are the creation and annihilation operators, which satisfy $[\hat{a}_\omega^\dagger, \hat{a}_\omega^\dagger] = 2\pi\delta(\omega - \omega\prime)$; $\mathcal{A}$ is the cross-sectional area of the optical beam; $u(x,y,z)$ is the spatial mode, satisfying $(1/\mathcal{A})\int dxdy|u(x,y,z)|^2 = 1$."[6] Now we define new operators $\hat{a}_1 = (\hat{a}_+ + \hat{a}_-^\dagger)/\sqrt{2}$ and $\hat{a}_2 = (\hat{a}_+ - \hat{a}_-^\dagger)/\sqrt{2}i$, the so-called amplitude and phase quadratures. These can be roughly interpreted as the amplitude and phase of the wave, however this is not true and in some cases leads to misinterpretation.[6] We can now rewrite the input electric field as:

$$\hat{E}(t)_{in} = [\sqrt{\frac{2I_0}{\hbar\omega_0}} + \hat{a}_1(t)]\cos(\omega_0 t) + \hat{a}_2(t)\sin(\omega_0 t) \tag{2}$$

The input beam then propagates through free space, making the output field the input field plus the time difference. Next we must solve to the amplitude and phase quadratures of the output field, $\hat{b}_1$ and $\hat{b}_2$ in terms of $\hat{a}_1$ and $\hat{a}_2$.

$$\hat{b}_1(t) = \hat{a}_1(t - 2\tau) \tag{3}$$

$$\hat{b}_2(t) = \hat{a}_2(t - 2\tau) - 2\sqrt{\frac{2I_0}{\hbar\omega_0}}\frac{\omega_0}{c}\hat{x}(t - \tau) \tag{4}$$

Now the equation of motion for the mass becomes the sum of the gravitational forces and the radiation pressure, $m\ddot{\hat{x}}(t) = \hat{F}_{rp}(t) + \frac{1}{2}mL\ddot{h}(t)$. Since the radiation pressure is known we may substitute

$$\hat{F}_{rp}(t) = \frac{2I_0}{c}[1 + \sqrt{\frac{2\hbar\omega_0}{I_0}}\hat{a}_1(t - \tau)] \tag{5}$$

From here, we compute the Fourier transform of $\hat{a}$,$\hat{b}$, and $\hat{x}$ from time to frequency and find the equation for $\hat{b}$ in terms of $\hat{a}$ and h. The component of $\hat{b}_2$ that is h (strain) dependent is the expectation value of $\hat{b}_2$, which we set equal to the transfer function times h.

$$\hat{b}_2(\Omega) = <\hat{b}_2(\Omega)> + \Delta\hat{b}_2(\Omega) \quad , \quad \Delta\hat{b}_2(\Omega) = e^{2i\Omega\tau}\hat{a}_2(\Omega) - \frac{8I_0\omega_0}{mc^2\Omega^2}e^{2i\Omega\tau}\hat{a}_1(\Omega) \tag{6}$$

The first part corresponds to the shot noise, depending on the phase fluctuations; while the second part is the radiation pressure noise, indicated by the amplitude fluctuations. Simply dividing by h gives the transfer function from the gravitational wave strain to the output phase quadrature:

$$\mathcal{T} = e^{i\Omega t}\sqrt{2\frac{I_0\omega_0 L^2}{\hbar c^2}} \tag{7}$$

Which allows us to solve for the spectral density of the quantum noise, our final result.

$$S^h(\Omega) = [\frac{1}{\xi I_0} + \xi I_0]\frac{h^2_{SQL}}{2} \tag{8}$$

Here it is easy to see the varying dependence of the shot noise and radiation pressure with optical power.

1.2.2 Discussion

Quantum noise is generated from an uncertainty in the phase of the outgoing laser. This uncertainty can be generated by two means: radiation pressure pushing on the mirror and adding small OPL changes or shot noise generated by uncertainty in the original phase generated by the laser. [6] It is important to note the major difference between our calculations in the previous section and reality. The derivation was for a simple Michelson interferometer, which means that there were no signal or power recycling mirrors involved. The most important difference between this derivation and reality for our purposes is that the shot noise would not have a flat spectrum, it will have a direct relationship with the frequency of the gravitational wave. This is because the similar uncertainties in phase are amplified by the recycling cavity. When that uncertainty is

amplified for higher frequency waves the uncertainty is much more comparable to the wavelength of a high frequency wave than that of a low frequency one. [6]

Equation (6) will be the most enlightening equation discussed in this section. Keep in mind that our goal is to reduce the quantum noise in the higher frequency range. Looking at our signal, it is composed of two parts, the signal and the noise. As previously stated the noise is composed of the shot noise and radiation pressure. One of the first observations we can make is that increasing the power in the laser will decrease the noise. Why? Immediately we can throw out the radiation pressure noise from our consideration because it is not the dominant noise at high frequencies. Turning our attention to the shot noise, it is proportional to $\frac{1}{\sqrt{N_\lambda}}$ [6], since the more individual trials (in this case photons) will gravitate towards the mean (the Law of Large Numbers). Therefore increasing the power should decrease the noise in the high frequency range; this is exactly what can be seen in our later computational optimization through differential evolution. [6] There are many variable that will effect the noise curve, and many are far less predictable than our brief analysis of power in this regard. This is why determining optimized parameters is left up to simulated differential evolution, to test numerous parameters simultaneously and locate the global minimum of the noise.

1.3 Substrate Brownian Noise

The substrate Brownian noise is generated from the mechanical dissipation of energy throughout the mass. Just like quantum noise, the noise is unavoidable, in this case because the mirror's temperature is nonzero. Just like in the case of quantum noise, it can be reduced after the mathematical derivation shows us how different variables change the noise spectrum.

1.3.1 Derivation

The derivation in this section follows the procedure developed by Levin. [13] It begins with the Fluctuation-Dissipation theorem from Callen and Welton [12]. This theorem shows that when there is one process dissipating energy in the form of heat, there is also a reverse process that can be quantified. The theorem is expressed mathematically as:

$$\mathcal{S}_x(f) = \frac{4l_B T}{\omega^2}\mathcal{R}](\mathcal{Z}) \tag{9}$$

Where $\mathcal{R}](\mathcal{Z})$ denotes the real portion of $\mathcal{Z}$, the impedance. A major part of the derivation is solving for this impedance, which is given by $\mathcal{Z} = \frac{v}{F}$. Where v is the velocity of the mirror and F is the force on the mirror. We begin by calculating the displacement of the mirror, given by the displacement of every point on the mass averaged by the intensity profile of the beam.

$$Z(t) = \int\int u_z(t,x,y)I(x,y)dxdy \tag{10}$$

The impedance is hidden in the calculation of $u_z(t,x,y)$. This part essentially assumes the force on the mirror to be oscillatory ($F = Fe^{i\omega t}$). It is then possible to calculate the position of each point on the mirror, and then compute its fourier transform. Then this substitution is made into equation 10, the real part is solved for.

$$\mathcal{Z}(f) = i\omega\frac{(1-i\phi)\int\int u_z(x,y)I(x,y)dxdy}{F} \tag{11}$$

$$\mathcal{R}e[\mathcal{Z}] = \omega\phi\frac{\int\int u_z(x,y)F \times I(x,y)dxdy}{F^2} \tag{12}$$

Noticing that the numerator is equivalent to the strain energy from elasticity theory allows a substitution which will simplify our spectral density quite nicely (here we define $U = \frac{W}{F^2}$ which normalizes the strain to 1N)[9]:

$$W = \frac{1}{2} \int \int u_z(x,y) p(x,y) dx dy \tag{13}$$

$$S_x(f) = \frac{4k_B T}{\pi f} \phi U \tag{14}$$

From here all that is left is to calculate the strain energy, which is a difficult task and material dependent. Levin has provided a calculation of U.[13]

$$S_x(f) = \frac{4k_B T}{f} \frac{1-\rho^2}{\pi^3 E_0 r_0} I \phi [1 + O(\frac{r_0}{R})] \tag{15}$$

Here E_0 and ρ are the Young's modulus and Poisson ratio of the material, respectively. I is the value 1.87322, and r_0 is the distance from the center of the beam to where it reaches $1/e$ intensity. The numerical values used by Gillespie and Raab for the remaining parameters are: $r_0 = 1.56$ cm, $E_0 = 57.183x1010$ Pa, $\rho = 0.16$, $\phi = 10^{-7}$, a mirror diameter of 25 cm, and a mirror length of 10 cm.

1.3.2 Discussion

The goal of this section was to derive the spectral density of the substrate thermal noise. This was done by applying an oscillatory force on the mirror, deriving the power dissipated throughout the test mass, and using these results to find the spectral density. It is given in two forms above, Equations 14 and 15. Just as in the discussion of Quantum noise, this allows us to make few simple observations. The spectral density has a direct relationship with temperature, and thus it would be advantageous to introduce cooling mechanisms to the substrate, an idea being implemented in the Einstein Telescope. [7] Turning our attention to the more involved Equation 15, it becomes less clear how certain parameters should change to improve sensitivity. One example is that the beam radius must be small relative to the mirror radius to reduce the correction term, while the beam radius must be maximized due to its inverse dependence in U.

Even if it were clear how certain parameters should change to reduce the thermal spectral density, these parameters have wide reaching consequences. It becomes advantageous to allow a software to calculate these dependencies and search for the optimal values within reason. This will be the focus of future sections.

2 A Modular and Adaptable Gravitational Wave Interferometer Noise Calculator

Deriving these simple formulas for noise is great, however in a real detector there are many more components than accounted for in our derivation. Therefore it becomes much more advantageous to allow a computer to calculate these spectral densities and their respective plots. For aLIGO, this software was called GWINC. Today, however, GWINC is not compatible with third generation detectors, prompting many to make the necessary modifications to allow the program to work. This leads to many individual programs derived independently, each with their own issues but more importantly: there is no standard software. This is the motivation behind MAGIC.

2.1 Validation of MAGIC

To prove the validity of MAGIC as a noise calculator, we first apply MAGIC to detectors with accepted noise curves. Comparisons of these noise curves for detectors such as aLIGO, Voyager, and ET will be presented as validation of MAGIC as a software. It will be shown that the MAGIC model for aLIGO and Voyager calculate valid noise curves, however there are some unknown issues with the Einstein Telescope calculations.

2.1.1 aLIGO

Being the oldest detector on this list, the curve for aLIGO is significantly more established. The two main discrepancies here are the peak in the accepted cuve does not appear in MAGIC's version, and MAGIC also has as a slightly higher noise in the 10-30 Hz range. The spike is likely due to some form of resonance being accounted for in the accepted model that MAGIC is not. The linearity of the second discrepancy indicates it is likely a thermal noise variation, and perhaps the models have different calculation parameters. Regardless, these variations are very slight; and it is clear that both curves are very similar.

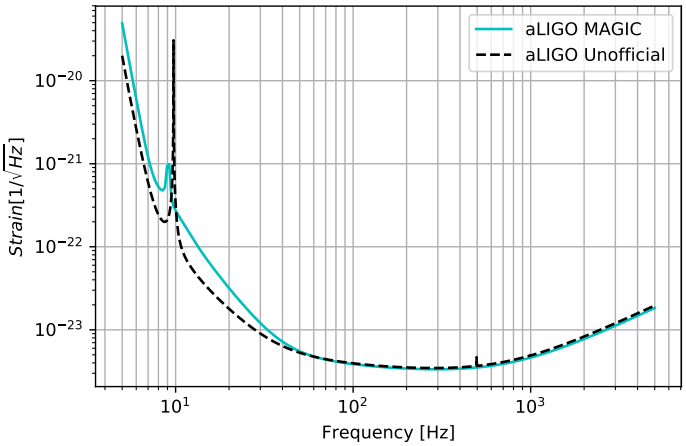

Figure 3: MAGIC aLIGO vs Accepted

2.1.2 Voyager

Voyager is exactly what MAGIC was built for, being the next generation detector in our horizons. This makes it a great test of the validity of the software. Here we can see that both curves are almost indistinguishable, save the small deviation in the low frequency bandwidth. This deviation, since it follows the accepted curve indicates that there is likely some linear factor with a varying parameter in the MAGIC model as compared to the accepted model. This is difficult to know without established parameters for Voyager, which are in flux as the design continues to be improved. Overall, this result is very welcome. This shows the MAGIC model is very capable of producing the same results as the accepted models.

2.1.3 ET

The Einstein Telescope model is going to be one of the most difficult to reproduce, and for a variety of reasons. Foremost, there is no true 'accepted' ET curve. There is, however it changes frequently due

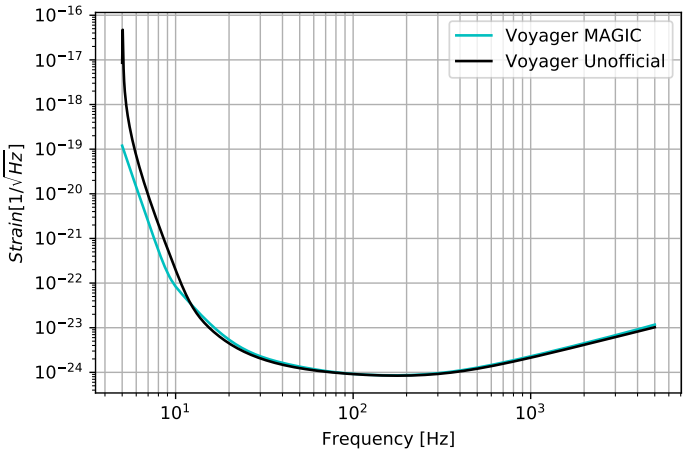

Figure 4: MAGIC Voyager vs Accepted

to advancements in the design. Even more difficult perhaps, there are no accepted parameters on which to build a model. Some things are solidified, yes, but many things change constantly as researchers work to improve the sensitivity. Even in light of these difficulties, the noise curves represented below are not close enough for a validation claim. The orders of magnitude difference could be explained by some dramatic difference in model parameters, but could also be explained some computational errors with the ET model in MAGIC. This will be evident once more during the application section on ET.

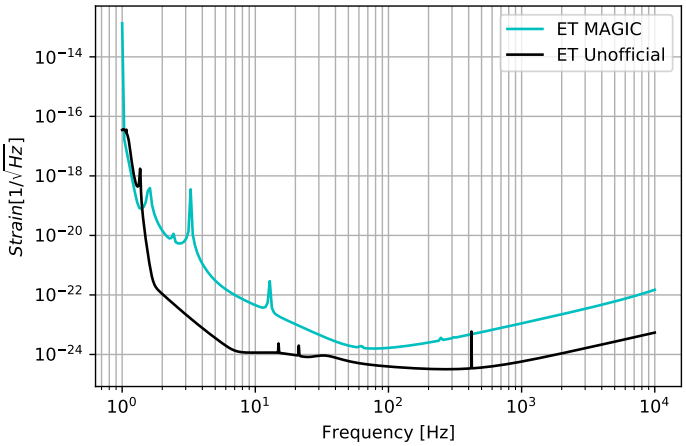

Figure 5: MAGIC ET vs Accepted

2.2 Application of MAGIC

2.2.1 DE-Optimization

Perhaps one of the more exciting features of MAGIC is not just the ability to graph noise curves, but its implementation of a brute force differential evolution optimization. This is something before unseen in the community. The current method requires a person to optimize parameters for a reduced noise, which is possible especially in the case of noise sources with predictable variations. However there are detector parameters that effect many noise sources unilaterally, such as the signal recycling cavity length. This makes it very difficult to predict the exact value which will reduce the noise as much as possible.

To solve this issue, MAGIC has implemented a differential evolution optimization. This metahuristic selects various candidate solutions (parameters for which the noise is minimized) and iteratively improves upon them, in an attempt to reach the global minimum of the integrated noise curve for a wide range of variable parameters. This function requires a strict guidance from the perspective of realistic engineering, however.

Left unchecked, the algorithm will select an infinitely massive mirror with an infinitely powerful laser. Thus bounds are set to procure realistic results. This was a simplistic example however because optimization with power as a parameter would be a pointless exercise. However it is important to note that various limits are set by what can realistically be done, and even if mathematically certain parameters might produce minimal noise they must be ruled out by such limits. This is something currently implemented within the software, however still requires careful oversight and reality-checks.

2.2.2 Optimization of Voyager

This section shows the validity of the differential evolution optimization tool with respect to Voyager. The detector was optimized for two different signals, binary black holes of 25 solar masses and of 1.4 solar masses. In both the metahuristic was capable of determining parameters with slightly lower noise curves. This serves as a fantastic example of the software being capable of determining slightly more optimal parameters. This calculation could almost certainly be improved upon by giving the differential evolution more parameters to optimize, however this will be more computationally expensive.

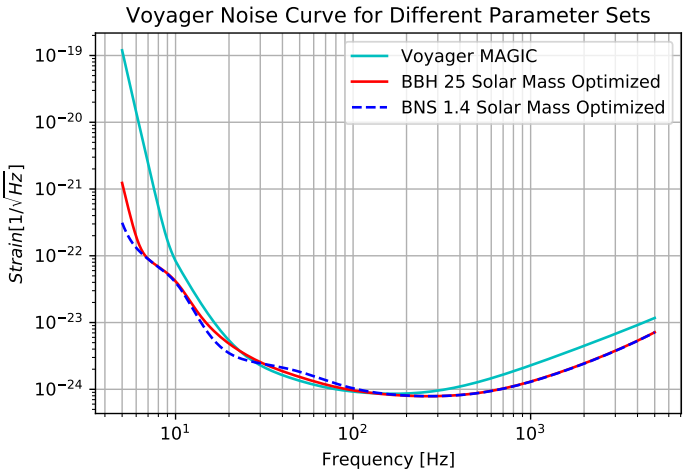

(a) Noise Curve

	25-25	1.4-1.4
Power (W)	298	300
Sus_len_4 (m)	1.16	2.55
Mass_4 (kg)	260	263
srm_transmittance	0.0238	0.0234

(b) Paramater Set

Figure 6: Voyager Optimized for Black Hole Binaries

2.2.3 Optimization of ET

Here it is important to note that something is incorrect with the ET model in MAGIC, as the sensitivity of the detector is certainly orders of magnitude off the correct noise curve. ET should be outperforming aLIGO and Voyager. Regardless, the model can still be used as evidence of the differential evolution capabilities. Here we optimize ET first as a single detector, in the model known as ET-120K (**??**). This is a single detector as opposed to the model usually considered where ET consists of two detectors optimized for high and low frequencies independently. The second variation is optimized in Figure (8).

Figure **??** shows once again the ability of differential evolution to improve upon the design slightly. It is able to remove the larger peaks in the low frequency range due to a change in suspension lengths (likely shifting the resonance frequencies). Figure 8 shows the ability of the program to optimize for low or high frequency detectors. The low frequency detector was optimized much more than the high frequency, likely due to the high frequency noise being shot noise restrained, and the laser power was invariant in the optimization. This shows that a differential evolution noise optimization will not always necessarily improve results, particularly when the set parameter boundaries do not allow for a reduction in the limiting noise source.

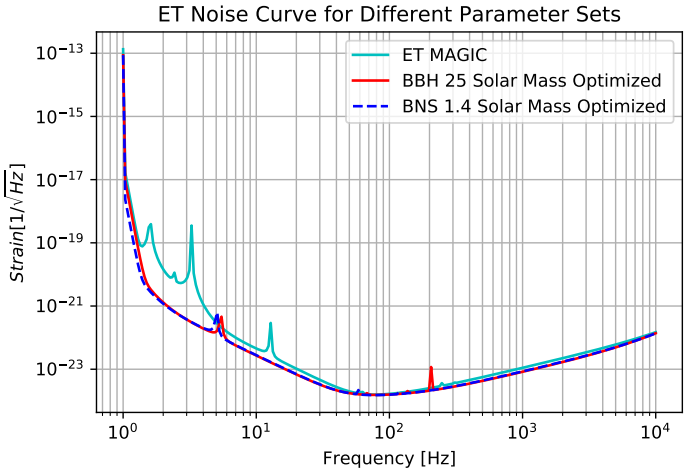

(a) Noise Curve

	25-25	1.4-1.4
Power (W)	300	300
Sus_len_4 (m)	1.59	1.85
Mass_4 (kg)	300	300
srm_trans mittance	0.038	0.040

(b) Paramater Set

Figure 7: ET Optimization for Binary Evolution

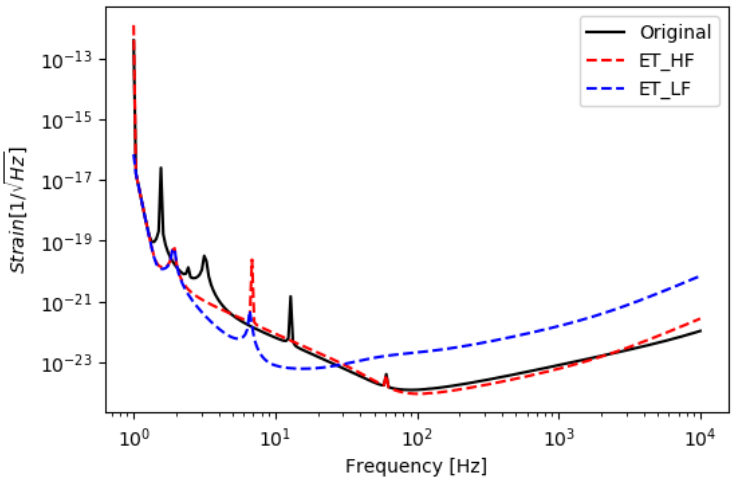

Figure 8: ET-LF and ET-HF Optimization

3 Conclusions

In the quest to construct the most accurate distance measuring device in existence, there are many different sources of interfering noise. These sources all have varying dependencies to a wide parameter set, making inferences about the effects of potential changes a difficult task. This paper began by deriving quantum noise, with the understanding that the results are not useful for an actual detector. Rather it gives an understanding of how noise spectral densities are formulated before being programmed, and why they need to be calculated computationally. Real detectors have far too many components to be calculated by hand, not that each individual step would be too difficult.

In both the quantum and thermal noise sections, it was shown that each source had some straightforward dependencies. The shot noise could be reduced by increasing the power, the radiation pressure noise could be reduced by increasing the mirror mass, and the substrate Brownian noise could be reduced by decreasing the temperature. However, they also had some apparently conflicting dependencies (ie shot noise is inversely proportional to power while radiation pressure noise is directly proportional to power).

For previous detectors there was a software for calculating these noise curves, called GWINC. As discussed, this software is out of date for next generation detectors. So the community is filled with various softwares attempting to solve the same issue with no formal standards. For this reason the University of Birmingham has developed a software called MAGIC[14, 15], in an attempt to prompt the discussion of a standardized noise calculator. MAGIC has been validated for detectors such as aLIGO and Voyager, however work still needs to be done on the Einstein Telescope model. The goal of MAGIC is not necessarily to be the standardized software in the community, but to start the conversation in working towards a standard.

MAGIC also introduces a new idea in the gravitational wave community, brute force differential evolution optimization of the detector. Rather than tuning parameters to reduce the dominant noise source, allowing a computer to calculate the global minimum of the integrated curve through brute force determination of optimal parameters. This process can become very computationally expensive without rigorously set parameter boundaries, and carefully selected parameters for optimization. The results of this work have verified MAGIC as a noise calculator, and have shown the ability of MAGIC's differential evolution toolkit to aid the community in choosing the precise parameter set for future gravitational wave detectors.

References

[1] Heaviside O. A gravitational and electromagnetic analogy,Electromagnetic Theory, 1893, vol.1 455 - 466 Appendix B

[2] Cervantes-Cota, J.L.; Galindo-Uribarri, S.; Smoot, G.F. (2016). "A Brief History of Gravitational Waves".

[3] Daniel Kennefick (29 March 2016). Traveling at the Speed of Thought: Einstein and the Quest for Gravitational Waves. Princeton University Press.

[4] Whittaker, Edmund Taylor (1910). A History of the theories of aether and electricity (1. ed.). Dublin: Longman, Green and Co.

[5] Bond, C., Brown, D., Freise, A. et al. Living Rev Relativ (2016) 19: 3. https://doi.org/10.1007/s41114-016-0002-8

[6] Haixing, Miao. Exploring Macroscopic Quantum Mechanics in Optomechanical Devices (2010)

[7] M Punturo et al 2010 Class. Quantum Grav. 27 194002

[8] B P Abbott et al 2009 Rep. Prog. Phys. 72 076901

[9] Vinet, Jean-Yves. "On Special Optical Modes and Thermal Issues in Advanced Gravitational Wave Interferometric Detectors." Living Reviews in Relativity, vol. 12, no. 1, 2009, doi:10.12942/lrr-2009-5.

[10] Coughlin, M, et al. "Towards a First Design of a Newtonian-Noise Cancellation System for Advanced LIGO." Classical and Quantum Gravity, vol. 33, no. 24, 2016, p. 244001., doi:10.1088/0264-9381/33/24/244001.

[11] Abernathy, M. "Einstein Gravitational Wave Telescope Conceptual Design Study." Letter of Intent, www.et-gw.eu/index.php/etdsdocument.

[12] Callen, H.B., and Welton, T.A., "Irreversibility and Generalized Noise", Phys. Rev., 83, 34-40, (1951).

[13] Levin, Y., "Internal thermal noise in the LIGO test masses: A direct approach", Phys. Rev. D, 57, $659 - 663$, (1998).

[14] Isobel Romero-Shaw, (2018) "A Modular and Adaptable Gravitational Wave Interferometer Noise Calculator"

[15] Roshni Vincent,(2018) "The use of a new Modular and Adaptable Gravitational wave Interferometer noise Calculator in Designing High Frequency Detectors"